university of groningen

Bachelor Research Project

Hippocampal Alterations in Alzheimer's Disease and the Modulatory Effects of TNF Alpha

Author: Froelich Matteo (S5121442)

Supervisor's: Wanda Douwenga, Giulia Mozzanica, and Jiahao Li

As part of the Uli Eisel group

Biology (BSc) with major in neuroscience (FSE)

April-May 2025

Abstract: Alzheimer's disease (AD) is a neurodegenerative disorder that impacts patients' memory and executive function. Characterized by amyloid-β (Aβ) plaques and neurofibrillary tau tangles, AD is extremely complex, involving many different mechanisms. A new player in this system is tumor necrosis factor-α (TNF-α), a cytokine that plays an antithetical role by promoting neuroprotection via its receptor 2 (TNFR-2) and neuroinflammation via its receptor 1 (TNFR-1). Previous research has associated TNF-α with the progression of AD, mainly attributing this to its inflammatory role, but given its dual signaling pathways, TNF-α represents a unique way to target neurodegeneration and neuroprotection pathways in AD. Accordingly, the aim of this study is to determine whether TNF-α modulation presents a viable and safe approach to combating AD. We began by assessing the effects of AD pathology on neuronal, synaptic, and oligodendrocyte markers in AD mouse model brains. Next, we explored the thermostability and cytotoxicity of a TNFR2 agonist, STAR2, using an MTT assay. Finally, the functional effects of a TNFR1 antagonist on J20 mice in a Y-maze were investigated. Our results were largely inconclusive; however, STAR2 appeared thermostable, while TNFR1 antagonism did not improve short-term memory in J20 mice. Still, given existing research, TNF-α modulation as a therapeutic for AD warrants further investigation to conclusively determine its potential disease-modifying effects.

"University of Groningen Corporate Logo." *University of Groningen*, 13 Jan. 2021, www.rug.nl/about-ug/practical-matters/huisstijl/logobank-new/corporatelogo/. Accessed 2 Apr. 2025.

Table of contents

1. Introduction

Alzheimer disease (AD) is the most common type of dementia, affects millions world-wide, and puts a major burden on the healthcare system, but is yet to see disease modifying treatments (Ortí-Casañ, Wajant, et al., 2023). With the hallmark of toxic amyloid-β (Aβ) aggregates and neurofibrillary tangles, patients with AD show degeneration of the hippocampus which leads to memory loss, and executive dysfunction.

Glial cells, such as astrocytes and microglia, play a phagocytic role in the central nervous system (CNS), responsible for uptake and degradation of Aβ peptides, but in AD these cells are dysregulated (Ortí-Casañ et al., 2022). With the overproduction of inflammatory signals, microglia are persistently activated leading them to inefficiently phagocytose Aβ. Among the many mediators of this chronic neuroinflammation tumor necrosis factor alpha (TNF-α) has emerged as a central driver of both microglial dysfunction and Aβ accumulation (Ortí-Casañ et al., 2019).

TNF-α is a pleiotropic cytokine found in cells across all tissues, acting as a key regulator of the immune system by mediating both pro- and anti-inflammatory pathways (Ortí-Casañ et al., 2019). In the CNS, TNF-α plays a dual roles in neuroinflammation and neuroprotection: binding to the tumor necrosis factor alpha 1 receptor (TNFR1) promotes apoptosis and inflammation, whereas engagement with the tumor necrosis factor alpha 2 receptor (TNFR2) supports neuroprotection by enhancing microglial phagocytosis and facilitating tissue repair (Ortí-Casañ et al., 2019; Ortí-Casañ et al., 2022). Indeed, as early as 1991, Dickson was among the first to report TNF-α expression in regions surrounding amyloid plaques. Later findings showed that TNF-α is initially expressed as a transmembrane protein (tmTNF) that can be cleaved into a soluble form (sTNF), with tmTNF mainly binding the TNFR2 and sTNF the TNFR1 (Aggarwal, 2000; Idriss and Naismith, 2000). Finally, research has shown that in the presence of ischemic lesions, TNFR2 deficient mice experience TNF-α–induced cell death, suggesting that TNFR1 signaling alone can drive neuronal damage (Fontaine et al., 2002). Furthermore, Fontaine et al. (2002) suggest that imbalances in TNF-α signaling, which are also observed in AD (Ortí-Casañ, Wajant, et al., 2023), exaggerate inflammatory responses that exacerbate cell death.

Current treatments for AD mainly provide symptomatic relief, without being disease-modifying or curative (Ortí-Casañ, Wajant, et al., 2023; Kim et al., 2024). Recent drugs such as aducanumab, lecanemab and donanemab primarily aim to reduce amyloid accumulation in an effort to alleviate symptoms and potentially improve cognitive function in AD (Kim et al., 2024). In contrast, a promising avenue of research is the pharmacological modulating TNF-α. By targeting this key upstream inflammatory pathway, it may be possible not only to utilize its neuroprotective effects but also to influence multiple aspects of the Alzheimer pathology, such as enhancing synaptic plasticity and improving microglial phagocytic activity (Ortí-Casañ et al., 2022; Ortí-Casañ, Wajant, et al., 2023).

Initial therapeutic strategies focused on globally inhibiting TNF-α; however, this approach often worsened neuroinflammation, likely due to the unintended suppression of TNFR2's protective effects (Fischer et al., 2015; Ortí-Casañ et al., 2019). More promising results have been found by inhibiting the TNFR1 receptor specifically, to dampen the neuroinflammatory response, while activating TNFR2 to enhance neuroprotection and restore microglia function (Ortí-Casañ et al., 2019). STAR2, a TNFR2 agonist, has been shown to restore balance in TNF-α signaling, enhancing microglial phagocytic activity and thereby promoting more efficient degradation of Aβ, ultimately leading to a reduction in plaques

(Ortí-Casañ et al., 2022). Similar results are found investigating Atrosimab, a TNFR1 antagonist with the ability to restore glial activity and reduce memory deficits in an acute neurodegenerative mouse model (Ortí-Casañ, Boerema, et al., 2023). However dose-dependent effects of STAR2 treatment, along with its chemical stability are yet to be studied. Furthermore, validating TNFR1 antagonism as a viable treatment in transgenic mouse models would provide additional evidence for the critical role of TNFR1 overactivation in Alzheimer's disease.

Accordingly, the current study aims to explore the therapeutic potential of TNF-α's dual role in AD with the following research question: Is TNF(-α) modulation a viable therapeutic approach to improve working memory in murine Alzheimer's disease models? The study will begin with immunohistochemical staining of brain tissue from both control and two AD mice models, namely J20 and triple transgenic (3xTg) mice. Synapsin-1, Olig-2 and NeuN will be stained to examine the impact of AD pathology on synaptic plasticity, oligodendrocyte density, and neuron density, respectively. Given the known synaptic and glial cell alterations in AD, we expect that Synapsin-1 and NeuN expression will be reduced, while Olig-2 expression may vary depending on disease stage and brain region (Benarroch, 2018; Kedia & Simons, 2025). Next, the thermal stability and cytotoxic effects of STAR2 treatment will be assessed using rhabdomyosarcoma kym-1 cells. Kym-1 cells are highly sensitive to TNF-α induced apoptosis, therefore effective STAR-2 treatment should result in cell death enabling assessment of the compound's stability at physiological temperature (Storz et al., 2000). Finally, a TNFR1 antagonist treatment will be tested using a standard Y-maze to explore its functional effects on working memory in AD and control mice.

2. Methods

2.1 Mice models

Mice samples for the immunohistochemical stainings and Y-maze videos were procured by University of Groningen. For staining, we employed J20 and 3xTg mice. J20 mice are genetically modified to overexpress the human amyloid precursor protein (via the expression of Swedish and Indiana mutations), resulting in recognizable AD characteristics, including amyloid plaque buildup, loss of synapses and neurons, and behavioral deficits (Karl et al., 2012; Hong et al., 2016; Tosh et al., 2018). Alternatively, 3xTg mice develop both amyloid plaque and neurofibrillary tangles in AD related brain areas (via the expression of $PS1_{M146V}$, APP_{SWE}, and tau_{P301L} mutations), also leading to cognitive deficits and reduction in synaptic plasticity (Oddo et al., 2003). For the control slices we used Groningen wild-type mice. Mice had access to food and water ad libitum and were on a 12:12 light/dark cycle. For the Y-maze experiments both male and female J20 mice were used. The behavioural tests were performed during the light phase of the cycle.

2.2 Immunohistochemical Staining for Olig-2

Coronal brain slices of WT, J20 and 3xTg samples stored in TBS 0.01M, were washed three times for 5min with TBS 0.01M pH 7.4 followed by 1h of pre-incubation in 3% BSA + 0.3% Triton-X in 0.001M TBS pH 7.4. Primary antibody incubation (1:500 rabbit anti-Olig-2) was done overnight at 4ºC on shaker in 3% BSA + 0.3% Triton-X in 0.001M TBS pH 7.4. A negative control was done by incubating with 3% BSA + 0.3% Triton-X in 0.001M TBS pH 7.4 instead of the primary antibody. Next, the samples were washed six times for 5 mins with TBS 0.01M pH 7.4. Working in the dark, secondary

antibody (1:400 donkey anti-rabbit-Alexa Fluor 488) incubation was done in 3% BSA + 0.3% Triton-X in 0.001M TBS pH 7.4 for 2hs at room-temperature. Samples were again rinsed three times for 5 mins with TBS 0.01M pH 7.4, and incubated overnight at 4ºC on shaker. Samples were mounted with mowiol antifade + DAPI.

2.3 Immunohistochemical Staining for NeuN

Coronal brain slices of WT, J20 and 3xTg samples stored in TBS 0.01M, were washed three times for 5min with TBS 0.01M pH 7.4 followed by 1h of pre-incubation in 5% BSA + 0.5% Triton-X in 0.001M TBS pH 7.4. Primary antibody incubation (1:500 mouse anti-NeuN) was done overnight at 4ºC on shaker in 5% BSA, 0.5% Triton-X in 0.001M TBS pH 7.4. A negative control was done by incubating with 5% BSA + 0.5% Triton-X in 0.001M TBS pH 7.4 instead of the primary antibody. Next, the samples were washed six times for 5 mins with TBS 0.01M pH 7.4. Working in the dark, secondary antibody (1:400 anti-rabbit Alexa Fluor 488) incubation was done in 5% BSA + 0.5% Triton-X in 0.001M TBS pH 7.4 for 2hs. Samples were again rinsed six times for 5 mins with TBS 0.01M pH 7.4, and incubated overnight at 4ºC on shaker. Samples were mounted with mowiol antifade + DAPI.

2.4 Immunohistochemical Staining for Synapsin-1

Coronal brain slices of WT, J20 and 3xTg samples stored in TBS 0.01M, were washed three times for 5min with TBS 0.01M pH 7.4 followed by 1h of pre-incubation in 5% Normal Donkey Serum (NDS), 0.5% Triton-X in 0.001M TBS pH 7.4. Primary antibody incubation (1:500 mouse anti-Synapsin-1) was done overnight at 4ºC on shaker in 3% BSA + 0.5% Triton-X in 0.001M TBS pH 7.4. A negative control was done by incubating with 5% Normal Donkey Serum (NDS), 0.5% Triton-X in 0.001M TBS pH 7.4 instead of the primary antibody. Next, the samples were washed six times for 5 mins with TBS 0.01M pH 7.4. Working in the dark, secondary antibody (1:400 anti-rabbit Alexa Fluor 488) incubation was done in 1% NDS + 0.3% Triton-X in 0.001M TBS pH 7.4 for 2hs. Samples were again rinsed six times for 5 mins with TBS 0.01M pH 7.4, and incubated overnight at 4ºC on shaker. Samples were mounted with mowiol antifade + DAPI.

2.5 Image analysis

Fluorescence images of the stainings were taken using a Leica DMi6000 Inverted Fluorescence Microscope at either a 10x or 20x magnification. The staining results were subsequently quantified using ImageJ software by measuring the percentage area of signal within the region of interest, specifically the hippocampus. This was achieved by making sure the image is in 16 bit and the threshold was adjusted so that as little background signal was present and as much signal of interest was isolated. These threshold settings were applied to all images of the same stain. The area of interest was selected using the polygon tool in ImageJ, and the percentage signal area was quantified using the 'Analyze' function. These values were then visualized graphically using RStudio.

2.6 Cytotoxicity Assay on Kym-1 cells

To test for the stability of the STAR2 a cytotoxicity assay was performed using an MTT assay in Kym-1 cells. Kym-1 cells were cultivated in RPMI medium supplemented with 1% penicillin streptomycin + 1% l-glutamine + 10% Fetal Bovine Serum (CO_2 incubator, 5%-10% CO_2). The Kym-1 cells ($1.5x10^4$ cells/well) were transferred to 96-well cell-culture plates and treated with 10, 100, or 1000

ng/ml of STAR2 stored at 4°C or 37°C. A total of 24 wells served as controls, with 6 wells allocated to each treatment condition. Cells were washed with PBS, then PBS with 5mg/ml MTT solution was added to each well followed by 2 hours of incubation (CO_2 incubator, 5%-10% CO_2). After discarding the supernatant, cells were stored at -80°C overnight. The following day, the plates were incubated at 37 °C for 30 minutes, after which 150 µl of DMSO was added. Absorbance was then recorded at 570 nm using a spectrophotometer.

2.7 Genotyping

Mouse tail snips were treated with 180 µL of buffer T1 and 25 µL of proteinase K, then incubated overnight at 56°C to be digested. Samples were centrifuged at 11,000 × g for 5 minutes to pellet remaining hair and bone fragments. The supernatant was transferred to a new tube containing 200 µL of buffer B3 and 210 µL of 100% ethanol. After vortexing, the mixture was incubated at 70°C for 10 minutes. DNA isolation was performed using spin columns: 500 µL of buffer BW and 600 µL of buffer B5 were added sequentially, each followed by centrifugation at 11,000 × g for 1 minute. After a dry spin, DNA was eluted with a preheated (70°C) elution buffer and collected by final centrifugation.

For PCR amplification, the master mix (per 20 µL reaction) contained 14.92 µL nuclease-free water, 2 µL DreamTaq buffer, 0.4 µL 10 mM dNTPs, 0.4 µL each of forward and reverse primers at 10 µM (see Table 1), 0.08 µL DreamTaq DNA polymerase, and 1 µL genomic DNA. PCR cycling conditions were: initial denaturation at 94°C for 2 minutes; 33 cycles of 94°C for 30 seconds (denaturation), 60°C for 30 seconds (annealing), and 72°C for 1 minute (extension); followed by a final extension at 72°C for 7 minutes. PCR products were separated on a 1% agarose gel run at 80 mA for 1 hour and visualized using a Chemidoc.

Table 1
Primers used for PCR

Identifier	Genotype	Primer	Sequence (5′-3′)
IMR8744	J20-negative	Forward	CAAATGTTGCTTGTCTGGTG
IMR8745	J20-negative	Reverse	GTCAGTGTCCACAGTTTG
IMR2044	J20 Transgene	Forward	GTGGAGTTTGTAAGTGATGCC
IMR2045	J20 Transgene	Reverse	TCTTCTTCTTCAACCTCAGC

2.8 Y-maze Video Analysis

To evaluate short-term working memory in J20 mice treated with either PBS or the TNFR1 antagonist, standard Y-maze videos were analyzed. In total, 23 videos were examined, including 12 from the TNFR1 antagonist group and 11 from the PBS-treated group. For ten minutes, each mouse was scored based on the sequence of arms it visited. A visit was confirmed when the mouse placed all four legs into the arm. With this, percentage alteration was calculated based on triads and total arm visits.

2.9 Statistical analysis

Statistical tests were performed using R-studio. For the MTT assay results, normality of the data was assessed using the Shapiro-Wilk test, and homogeneity of variances was checked with Levene's test. Based on these results, the personal results were analysed using a two-way ANOVA paired with a Tukey's multiple comparisons post-hoc test. Given the non-parametric distribution of the grouped data a two-way Aligned Rank Transform ANOVA (ART-ANOVA) was performed, combined with a Tukey's multiple comparisons post-hoc test. Additionally, a Pearson's R correlation test was performed to see if a linear relation was present between the concentration and cell viability. A student's t-test was performed on the Y-maze video results to compare groups, and a two-way ANOVA to test sex-dependent interactions. Statistical significance was accepted at $p < 0.05$. All data are presented as mean ± standard error of the mean (SEM).

3. Results

3.1 Immunohistochemistry resulted in unclear signal, leading to no significant results

To assess baseline effects of Alzheimer's disease pathology on synaptic plasticity along with oligodendrocyte and neuronal cell densities, immunofluorescent staining was performed on brain sections from WT, J20, and 3xTg mice. DAPI staining was successful in all samples, allowing clear recognition of the hippocampus and individual nuclei. Negative controls for Olig-2 and Synapsin-1 worked as expected, but high background noise limits the comparison between groups (Fig. 1A-B). However, NeuN showed strong background with signal levels of the negative control matching those in stained samples (Fig. 1C).

Synapsin-1 staining appears more intense within the region enclosed by the dentate gyrus (highlighted in white in Fig. 1B), compared to surrounding areas. Furthermore, the enlarged images of the 3xTg Olig-2 staining (Fig. 1E) show possible oligodendrocytes signals as indicated by the red arrow. These signals partially overlap with DAPI since Olig-2 labels nuclear transcription factors and DAPI stains all nuclei. Despite these observations, quantitative analysis of signal area percentages (Fig. 1D) showed unexpected trends: 3xTg mice exhibited the highest Olig-2 signal, while J20 mice showed the highest Synapsin-1 signal.

3.2 Increasing Star2 concentration leads to decreased cell viability in kym-1 cells

To evaluate the cytotoxic effects and thermostability of the TNFR2 agonist STAR2, a MTT assay was performed on Kym-1 cells using a range of concentrations (10, 100, 1000 ng/ml) and samples stored at 4 °C and 37 °C. Given that Kym-1 cells are prone to TNFR2-mediated apoptosis, it was expected that increasing concentrations of STAR2 would reduce cell viability. This trend was partially supported by the results (Fig. 2A-C). Although not statistically significant, grouped data (Fig. 2A) showed a strong negative correlation of 37°C stored STAR2 ($r = -0.97$, $p = 0.16$) and a moderate negative correlation for the 4°C ($r = -0.72$, $p = 0.49$).

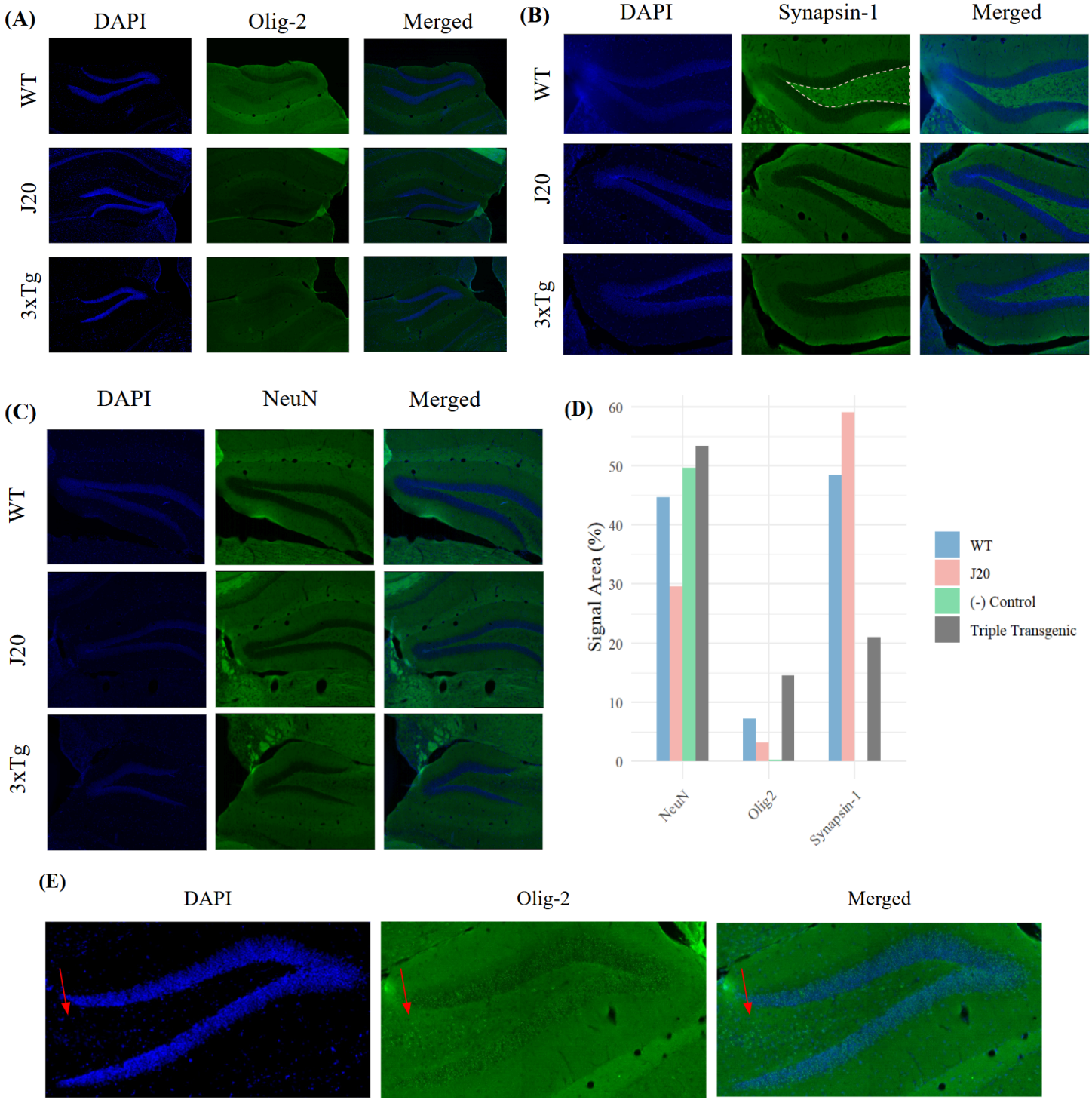

Figure 1: WT and AD models showed similar hippocampal staining. (A) Sections were stained with DAPI (blue) for nuclei and Fluor-488 (green) for Olig-2. (B) Sections were stained with DAPI (blue) to label nuclei and Fluor-488 (green) to detect Synapsin-1. The region outlined in white shows a darker green signal for every treatment, potentially indicating Synapsin-1 expression. (C) Sections were stained with DAPI (blue) for nuclei and Fluor-488 (green) for Synapsin-1. (D) Quantification of percentage signal area coverage for a single sample of each marker. (E) Enlarged 3xTG Olig-2 staining reveals possible oligodendrocyte signals in the area indicated by the red arrow.

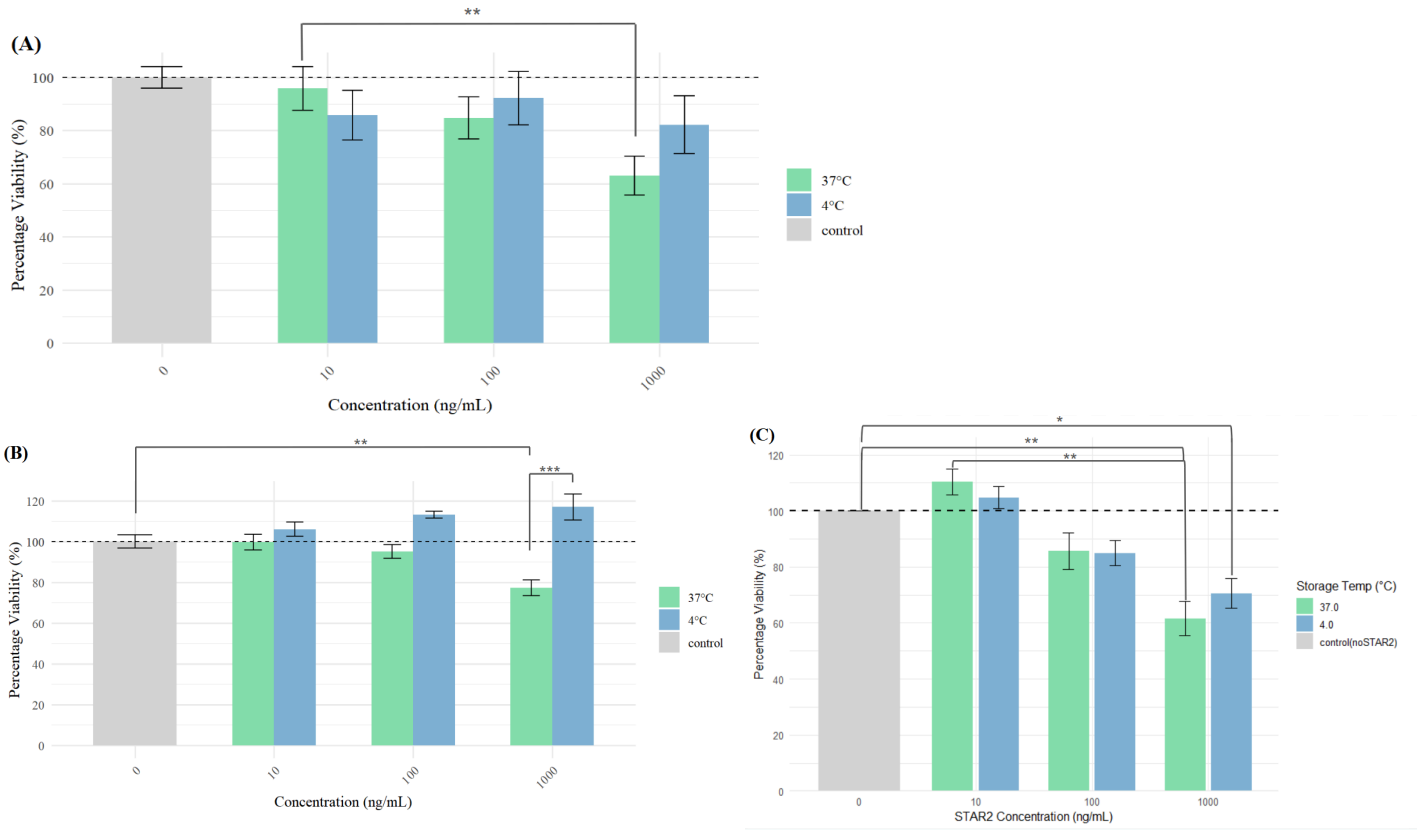

Figure 2: STAR2 reduces kym-1 cell viability. (A) Grouped MTT assay results show a significant reduction in viability at 1000 ng/mL compared to 10 ng/mL ($p = 0.0019$) (control, n= 168; per treatment, n= 42; two-way ART-Anova with Tukey post-hoc analysis). (B) Personal MTT assay results show a significant decrease in cell viability at 1000 ng/mL STAR2 under 37°C conditions compared to control ($p= 0.0051$), while under 4°C conditions, percentage viability values exceed 100% (control, n = 24; per treatment, n = 6; two-way ANOVA with Tukey's post hoc analysis). (C) Leon's MTT assay results show a significant reduction in cell viability with 1000 ng/ml STAR treatment stored at both 37°C ($p = 0.0012$) and 4°C ($p = 0.025$) compared to control. However, at 10 ng/ml values exceeding 100% are observed for both temperature treatments (control, n = 24; per treatment, n = 6; two-way ANOVA with Tukey's post hoc analysis). Data are presented as mean ± SEM. *$p < 0.05$; **$p < 0.01$; *** $p < 0.001$.

My personal results (Fig. 2B) show a statistically significant negative correlation with the 37°C stored version STAR2 ($r = -0.76$, $p = 0.0003$), but a positive correlation with the 4°C stored version ($r = 0.347$, $p = 0.16$). This positive correlation in the 4°C is likely due to the contamination, as indicated by cell viability values exceeding 100%, suggesting that this experiment was compromised. Therefore any significant correlations should be interpreted with caution, as contamination also affected the control group used as a reference.

In contrast, Leon's plate (Fig. 2C) showed no signs of contamination and displays a significant negative trend in cell viability with increasing STAR2 concentrations at both 37°C ($r = –0.754$, $p = 0.00030$) and 4°C ($r = –0.692$, $p = 0.00146$). However, both storage conditions at 10 ng/mL showed

viability values exceeding 100% likely due to pipetting errors, raising concerns about the reliability of these specific data points. Overall, Kym-1 cell viability appears to decrease with increasing STAR2 concentration, while storage temperature shows no significant effect.

3.3 TNFR1 antagonism has no behavioural effects in a Y-maze with J20 mice

To assess the impact of TNFR2 agonist treatment on short-term working memory, Y-maze videos of J20 mice treated with either the agonist or PBS were analyzed. Analysis of results by treatment ($p = 0.43$) and by sex (male $p = 0.12$; female, $p = 0.5$) show no significant results (Fig. 3A-B). Furthermore, a two-way ANOVA revealed no sex-dependent interaction effect on treatment ($p = 0.13$). Overall, these findings suggest that TNFR2 agonist treatment did not significantly influence working memory in a standard Y-maze.

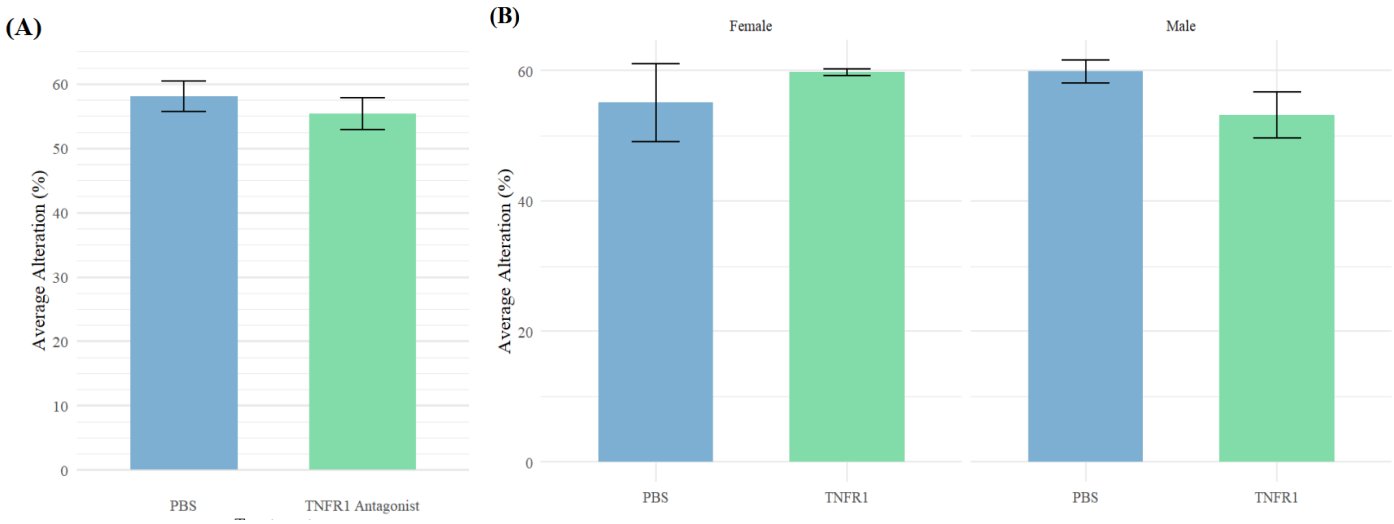

Figure 3: TNFR1 treated J20 mice behave similarly as control. (A) Quantification by treatment shows no significant difference between treatments ($p = 0.43$) (PBS, n=12; TNFR1 Antagonist, n=11; unpaired t-test). (B) Similarly, separation by sex shows no significant difference (male, $p = 0.12$; female, $p = 0.5$; unpaired t-test) with no treatment × sex interaction interaction (male, n=15; female, n=8; $p = 0.13$, two-way ANOVA). Data are presented as mean ± SEM.

4. Discussion

To investigate whether TNF-α modulation can influence Alzheimer's disease progression, three independent experiments were conducted. An initial immunofluorescent staining was performed on brain sections from wild-type (WT) mice and two Alzheimer's disease models, 3xTg and J20, staining for NeuN, Synapsin-1, and Olig-2. This aimed to provide insight into the impact of Alzheimer's disease pathology on key neurobiological processes, including synaptic plasticity and oligodendrocyte density. Next, an MTT assay was conducted on Kym-1 cells to evaluate the cytotoxic effects of a TNFR2 agonist, STAR2. Different concentrations of the compound were tested, along with samples stored at 4°C and 37°C to assess its thermostability. Lastly, Y-maze videos were analysed to assess the effect of a TNFR1 antagonist on short-term working memory of J20 mice. Overall, the current study yielded inconclusive

results regarding both AD-related pathological markers and the viability of TNF-α modulating drugs to improve AD progression.

Immunofluorescence stainings were largely unsuccessful in determining differences in synaptic plasticity, neuronal density and oligodendrocytes density between AD mice models and WT controls. NeuN staining yielded high levels of background noise that were indistinguishable from positive signals, as exemplified by the comparable percentage signal area of the positive control compared to the experimental samples (Fig. 1D). Synapsin-1 staining shows possible signals, indicated by a white outline (Fig. 1B), which appear consistently across groups and are more prominent in the area enclosed by the dentate gyrus. These findings are consistent with previous research, where mossy fibres, with unusually large synapses (named mossy fibre boutons), originate from the inner DG and project to the CA3 (Rollenhagen et al., 2007). These mossy fibres also exhibit particularly high levels of synaptic plasticity, which would explain the higher intensity stain in the inner DG region (Rollenhagen et al., 2007; Shahoha et al., 2022). Furthermore, a study by Herrmann et al. (2012) reported similar findings, demonstrating that synapsin-1 is predominantly expressed in the CA3/hilus and dentate gyrus regions[1] of the mouse hippocampus.

Based on the expected severity of AD-related pathology, we hypothesized that synaptic plasticity would be highest in wild-type (WT) mice, intermediate in J20 mice, and lowest in 3xTg mice. AD is known to negatively impact synaptic plasticity through Aβ oligomers, which bind to presynaptic and postsynaptic sites (Benarroch, 2018). Consequently, Aβ accumulation decreases long-term potentiation leading to decreased densities of dendritic spines in several mouse models. Furthermore, 3xTg are also exposed to neurofibrillary tangles which are also known to negatively impact synaptic plasticity (Tracy et al., 2016). However, these expectations were not met likely due to high background levels of nonspecific antibody binding, as indicated by only a faint difference in staining density between the inner and outer dentate gyrus (Figure 1B).

Similarly, the Olig-2 staining (Fig. 1A) showed potential positive signals but comparison across groups was unsuccessful due to the low clarity of the signals. Previous studies have shown that Olig-2 staining is expected to produce positive signals in the inner dentate gyrus (CA4), similar to the pattern observed with Synapsin-1, which is consistent with our findings (DeFlitch et al., 2022). Additionally, since Olig-2 is a nuclear transcription factor, Olig-2 positive stainings should colocalize with DAPI. However, this overlap is only partially present in our samples, questioning the validity of the staining results. When analyzing staining intensities across groups our results did not align with previous research.

Oligodendrocytes are known to be negatively affected by AD pathology, but it is important to consider the timing of these changes. Early on, oligodendrocytes of AD models increase proliferation compared to controls (Kedia & Simons, 2025), possibly as a response to increased inflammation. However, Solène Ferreira et al. (2020) reported that newly generated oligodendrocytes appear to compensate for those lost, resulting in no change in the total oligodendrocyte population up to 5–6 months of age in APP transgenic mice. After this 5-6 month threshold, oligodendrocyte populations are known to significantly decrease, especially in the inner dentate gyrus (DeFlitch et al., 2022). Therefore, depending

[1] Notation of the area enclosed by the dentate gyrus has several names, such as the inner dentate gyrus; hilus; CA4 area. In this research paper, this area is referred to as the inner dentate gyrus.

on the age of the mice, differences in Olig-2 signal intensity may not be expected. However, our results indicate that 3xTg mice exhibited the highest oligodendrocyte population (Fig. 1D), and even if these were young mice, such findings are unexpected.

The lack of consistent results in the immunofluorescence stainings can be explained by the low binding efficiency of the antibodies used. Exactly why these antibodies bound sub-optimally is difficult to determine given the many factors at play. It could be due to human error, such as missing a washing step which would increase the chances of unspecific binding or to a procedural inconsistency. For example, the antibodies may have not been specific enough to the target of interest, increasing background noise. Additionally, only one sample was quantitatively analyzed for each staining, making between group analysis unreliable, and no positive control was employed. A positive control could involve staining for a known structure, such as the housekeeping protein tubulin, to control for procedural errors.

The MTT cytotoxicity assay showed that STAR2 overall lowers cell viability (Fig. 2A-C), with storage temperature having no significant effect. Kym-1 cells are known to undergo TNFR1 mediated apoptosis (Storz et al., 2000), therefore such a negative trend in cell viability with increasing STAR2 concentration indirectly confirms TNFR2 binding by STAR2. Furthermore, other than my personal plate (Fig. 2B), which is not valid due to the high amount of contamination present, the MTT assay shows that STAR2 stored at 37°C results in a similar trend as the correctly 4°C stored version. This somewhat confirms STAR2's thermostability, as it retains its ability to bind TNFR2 even after being stored at physiological temperature for several months.

However, this conclusion is uncertain, as improperly stored STAR2 may also induce cell death through alternative pathways, the effects of which are masked by its primary TNFR2-induced apoptosis. Furthermore, given that pharmaceutical proteins can degrade at higher temperatures into toxic by-products, clarifying STAR2's cytotoxicity is essential (Akbarian & Chen, 2022). This could be done by using a negative control cell line that does not readily undergo TNFR2-induced apoptosis alongside Kym-1 cells. Ideally, a genetically modified Kym-1 cell line lacking TNFR2 (TNFR2 knockout) would provide even deeper insights of STAR2's potential cytotoxic effects.

Lastly, the Y-maze videos showed that TNFR1 antagonist treatment has no effect on the short-term working memory of J20 mice. Although unexpected, these results are consistent with previous research. The standard Y-maze evaluates short-term working memory, which involves the hippocampus but also the ventral striatum and prefrontal cortex (Ortí-Casañ, Boerema, et al., 2023). In J20 mice, mainly the hippocampus is affected by Aβ accumulation, while other brain areas remain functionally intact. Therefore, by testing short-term working memory we hypothesize that other brain areas, namely the VS and PFC, can compensate for the loss of hippocampal function. Indeed, in similar experiments other researchers utilize the Y-maze as a baseline test to assure that all subjects have an unimpaired working memory (Ortí-Casañ, Boerema, et al., 2023). To better evaluate the memory of these mice, hippocampus dependent long-term memory tests, such as the Morris Water Maze and Passive Avoidance test, should be carried out.

5. Conclusion

The current study set out to determine the effects of AD pathology on mice hippocampus and to evaluate whether TNF-α modulation represents a viable therapeutic strategy for improving such AD-related deficits. No effect of AD pathology was found when staining for specific markers, but an MTT cytotoxicity assay confirmed a dose-dependent negative effects of STAR2, a TNFR2 agonist, on kym-1 cell viability. The thermostability of STAR2 should still be explored in future research using a negative control. Lastly, the Y-maze conducted on J20 mice treated with a TNFR1 antagonist revealed no significant differences because such a behavioural test evaluates short-term working memory. These findings support future research on the potential of targeting TNF-α to alter the effects AD has on millions of patients worldwide. Future research should explore how TNFR1 and TNFR2 modulation affects both neuropathological markers and behavior in AD mouse models.

Declaration of AI use: ChatGPT was used to improve the readability of existing text and to assist with R-Studio coding. It helped identify certain relevant sources, but no content generated by the model was directly used in the report.

6. References

Aggarwal, B. B. (2000). Tumour necrosis factors receptor associated signalling molecules and their role in activation of apoptosis, JNK and NF-κB. *Annals of the Rheumatic Diseases*, *59*, i6–i16. https://doi.org/10.1136/ard.59.suppl_1.i6

Akbarian, M., & Chen, S.-H. (2022). Instability challenges and stabilization strategies of pharmaceutical proteins. *Pharmaceutics*, *14*(11), 2533. https://doi.org/10.3390/pharmaceutics14112533

Benarroch, E. E. (2018). Glutamatergic synaptic plasticity and dysfunction in Alzheimer disease. *Neurology*, *91*(3), 125–132. https://doi.org/10.1212/wnl.0000000000005807

DeFlitch, L., Gonzalez-Fernandez, E., Crawley, I., & Kang, S. H. (2022). Age and alzheimer's disease-related oligodendrocyte changes in hippocampal subregions. *Frontiers in Cellular Neuroscience*, *16*. https://doi.org/10.3389/fncel.2022.847097

Dickson, D. W. (1997). The pathogenesis of senile plaques. *Journal of Neuropathology and Experimental Neurology*, *56*(4), 321–339. https://doi.org/10.1097/00005072-199704000-00001

Herrmann, L., Ionescu, I. A., Henes, K., Golub, Y., Wang, N. X. R., Buell, D. R., Holsboer, F., Wotjak, C. T., & Schmidt, U. (2012). Long-Lasting hippocampal synaptic protein loss in a mouse model of posttraumatic stress disorder. *PLoS ONE*, *7*(8), e42603. https://doi.org/10.1371/journal.pone.0042603

Hong, S., Beja-Glasser, V. F., Nfonoyim, B. M., Frouin, A., Li, S., Ramakrishnan, S., Merry, K. M., Shi, Q., Rosenthal, A., Barres, B. A., Lemere, C. A., Selkoe, D. J., & Stevens, B. (2016). Complement and microglia mediate early synapse loss in Alzheimer mouse models. *Science*, *352*(6286), 712–716. https://doi.org/10.1126/science.aad8373

Idriss, H. T., & Naismith, J. H. (2000). TNFa and the TNF receptor superfamily: Structure-function relationship(s). *Microscopy Research and Technique*, *50*(3), 184–195. https://doi.org/10.1002/1097-0029(20000801)50:3<184::aid-jemt2>3.0.co;2-h

Karl, T., Bhatia, S., Cheng, D., Kim, W. S., & Garner, B. (2012). Cognitive phenotyping of amyloid precursor protein transgenic J20 mice. *Behavioural Brain Research*, *228*(2), 392–397. https://doi.org/10.1016/j.bbr.2011.12.021

Kedia, S., & Simons, M. (2025). Oligodendrocytes in Alzheimer's disease pathophysiology. *Nature Neuroscience*, *28*(3), 446–456. https://doi.org/10.1038/s41593-025-01873-x

Kim, A. Y., Al Jerdi, S., MacDonald, R., & Triggle, C. R. (2024). Alzheimer's disease and its treatment–yesterday, today, and tomorrow. *Frontiers in Pharmacology*, *15*. https://doi.org/10.3389/fphar.2024.1399121

Oddo, S., Caccamo, A., Shepherd, J. D., Murphy, M. P., Golde, T. E., Kayed, R., Metherate, R., Mattson, M. P., Akbari, Y., & LaFerla, F. M. (2003). Triple-Transgenic model of alzheimer's disease with plaques and tangles. *Neuron*, *39*(3), 409–421. https://doi.org/10.1016/s0896-6273(03)00434-3

Ortí-Casañ, N., Boerema, A. S., Köpke, K., Ebskamp, A., Keijser, J., Zhang, Y., Chen, T., Dolga, A. M., Broersen, K., Fischer, R., Pfizenmaier, K., Kontermann, R. E., & Eisel, U. L. M. (2023). The TNFR1 antagonist Atrosimab reduces neuronal loss, glial activation and memory deficits in an acute mouse model of neurodegeneration. *Scientific Reports*, *13*(1). https://doi.org/10.1038/s41598-023-36846-2

Ortí-Casañ, N., Wajant, H., Kuiperij, H. B., Hooijsma, A., Tromp, L., Poortman, I. L., Tadema, N., de Lange, J. H. E., Verbeek, M. M., De Deyn, P. P., Naudé, P. J. W., & Eisel, U. L. M. (2023). Activation of TNF receptor 2 improves synaptic plasticity and enhances amyloid-β clearance in an alzheimer's disease mouse model with humanized TNF receptor 2. *Journal of Alzheimer's Disease*, *94*(3), 977–991. https://doi.org/10.3233/jad-221230

Ortí-Casañ, N., Wu, Y., Naudé, P. J. W., De Deyn, P. P., Zuhorn, I. S., & Eisel, U. L. M. (2019). Targeting TNFR2 as a novel therapeutic strategy for alzheimer's disease. *Frontiers in Neuroscience*, *13*. https://doi.org/10.3389/fnins.2019.00049

Ortí-Casañ, N., Zuhorn, I. S., Naudé, P. J. W., De Deyn, P. P., van Schaik, P. E. M., Wajant, H., & Eisel, U. L. M. (2022). A TNF receptor 2 agonist ameliorates neuropathology and improves cognition in

an Alzheimer's disease mouse model. *Proceedings of the National Academy of Sciences*, *119*(37). https://doi.org/10.1073/pnas.2201137119

Rollenhagen, A., Sätzler, K., Rodríguez, E. P., Jonas, P., Frotscher, M., & Lübke, J. H. R. (2007). Structural determinants of transmission at large hippocampal mossy fiber synapses. *The Journal of Neuroscience*, *27*(39), 10434–10444. https://doi.org/10.1523/jneurosci.1946-07.2007

Shahoha, M., Cohen, R., Ben-Simon, Y., & Ashery, U. (2022). cAMP-Dependent Synaptic Plasticity at the Hippocampal Mossy Fiber Terminal. *Frontiers in Synaptic Neuroscience*, *14*. https://doi.org/10.3389/fnsyn.2022.861215

Solène Ferreira, Kimberley A. Pitman, Shiwei Wang, Benjamin S. Summers, Nicole Bye, Kaylene M. Young, & Carlie L. Cullen. (2020). Amyloidosis is associated with thicker myelin and increased oligodendrogenesis in the adult mouse brain. *J Neurosci Res.*, *98*(10). https://doi.org/10.1002/jnr.24672

Storz, P., Döppler, H., Horn-Müller, J., Müller, G., & Pfizenmaier, K. (2000). TNF down-regulation of receptor tyrosine kinase-dependent mitogenic signal pathways as an important step in cytostasis induction and commitment to apoptosis of Kym-1 rhabdomyosarcoma cells. *Cell Death & Differentiation*, *7*(10), 955–965. https://doi.org/10.1038/sj.cdd.4400732

Tosh, J. L., Rickman, M., Rhymes, E., Norona, F. E., Clayton, E., Mucke, L., Isaacs, A. M., Fisher, E. M. C., & Wiseman, F. K. (2018). The integration site of the APP transgene in the J20 mouse model of Alzheimer's disease. *Wellcome Open Research*, *2*, 84. https://doi.org/10.12688/wellcomeopenres.12237.2

Tracy, T. E., Sohn, P. D., Minami, S. S., Wang, C., Min, S.-W., Li, Y., Zhou, Y., Le, D., Lo, I., Ponnusamy, R., Cong, X., Schilling, B., Ellerby, L. M., Huganir, R. L., & Gan, L. (2016). Acetylated tau obstructs kibra-mediated signaling in synaptic plasticity and promotes tauopathy-related memory loss. *Neuron*, *90*(2), 245–260. https://doi.org/10.1016/j.neuron.2016.03.005

7. *Supplementary figures*

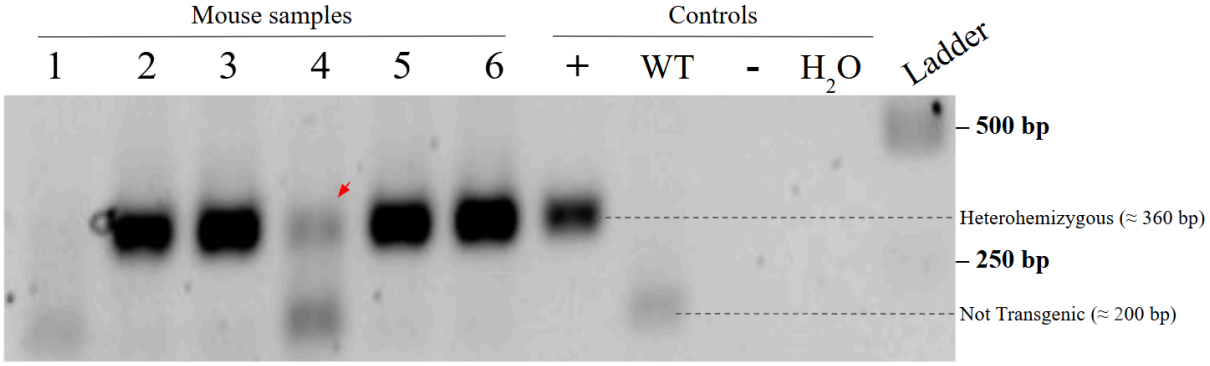

Figure 1: Gel electrophoresis results of the genotyping carried out before Y-maze analysis. Red arrow indicates unexpected contamination of a transgenic into a WT sample upon pipetting the well. The 200 bp band, representing a wild-type amplified gene also present in transgenic mice, was expected in all samples but appears only in WT due to primer competition. Mouse samples 1 and 4 are WT, while 2,3,5 and 6 are J20.

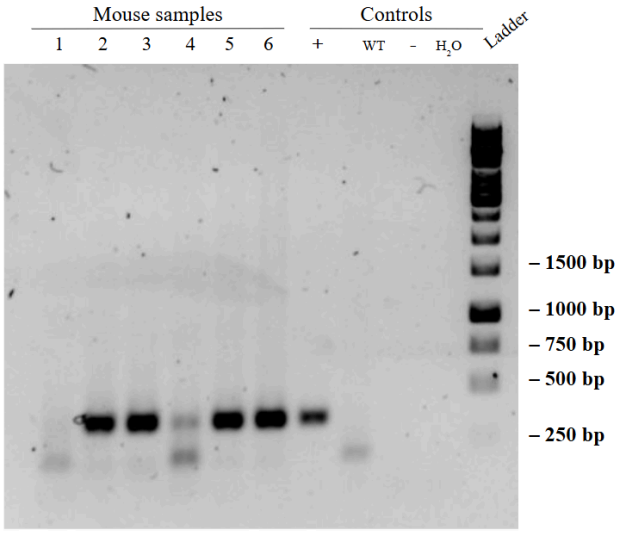

Figure 2: Full gel image